

COMBUSTION STUDIES ON CONCENTRATED DISTILLERY EFFLUENTS

N. M. PATEL, P. J. PAUL, H. S. MUKUNDA AND S. DASAPPA

*Department of Aerospace Engineering
Indian Institute of Science
Bangalore—560 012, India*

Studies on ignition and combustion of distillery effluent containing solids consisting of $38 \pm 2\%$ inorganics and $62 \pm 2\%$ of organics (cane sugar derivatives) have been carried out in order to investigate the role of droplet size and ambient temperature in the process of combustion. Experiments were conducted on (1) liquid droplets of effluent having solids concentration 65% and (2) spheres of dried (100% solids) effluent of diameters ranging from 0.5 to 25 mm. These spheres were introduced into a furnace where air temperature ranged from 500 to 1000 °C, and they burned with two distinct regimes of combustion—flaming and glowing. The ignition delay of the 65% concentration effluent increases with diameter as in the case of nonvolatile droplets, while that of dried spheres appears to be independent of size. The ignition delay shows Arrhenius dependence on temperature. The flaming combustion involves a weight loss of 50–80%, depending on ambient temperature, and the flaming time is given by $t_f \sim d_0^2$, as in the case of liquid fuel droplets and wood spheres. Char glowing involves weight loss of an additional 10–20%, with glowing time behaving as $t_c \sim d_0^2$ as in the case of wood char, even though the inert content of effluent char is as large as 50% compared to 2–3% in wood char. Char combustion has been modeled, and the results of this model compare well with the experimental results.

Introduction

All distilleries produce an effluent commonly known as “vinasse,” an amount equal to 10–15 times that of the volume of alcohol. Dry vinasse or effluent contains about 38–40% inorganic salts of potassium, sodium, magnesium, and calcium in the form of chlorides, sulfates, and phosphates, and about 60–62% organic compounds, in particular, sugar (cane sugar, $C_{12}H_{22}O_{11}$). Besides a strong pungent smell and intense dark color, effluent has a large biological oxygen demand (BOD) and chemical oxygen demand (COD) in the range of 45 and 100 g/L, respectively, and hence, the effluent is included in the list of highly polluting chemicals. Among the methods of effluent disposal, biomethanation and incineration of concentrated effluent are the options. In the biomethanation route, biogas digesters convert the organic matter into methane and carbon dioxide. However, the discharged effluent from the biogas plant still has unacceptable levels of BOD to allow discharge into land or river. Other routes, such as biocomposting, are contemplated in order to dispose the effluent safely. Yet, there have been considerable difficulties in meeting the rigorous pollution standards. Considering the incineration route, all the organic matter can be treated, and the inorganic matter, amounting to 6–7% of the effluent, needs to be disposed. This material can be used as a fertilizer. Another route along incineration process is the gasification of concentrated effluent. This process can

be described as substoichiometric combustion, in which oxidation reactions between the organic matter and oxygen in the oxidant (air), and reduction reactions between the products of combustion and unconverted carbon, lead to the generation of a combustible gas called producer gas containing CO, H₂, CH₄, CO₂, and N₂. This can be used as a fuel in an internal combustion engine or gas turbine in single fuel or dual-fuel mode to generate electricity. Hence, this method provides power while having zero effluent discharge. This process has been addressed inadequately and the limited field experience available on this technique at present has been negative. One of the issues is that the fundamental process associated with incineration and gasification aspects of effluent has not been understood. One phase of combustion, namely, the flaming combustion during which the volatile matter is oxidized in air, is common to both combustion and gasification. During the second phase, carbon reacts with oxygen in case of combustion and with CO₂ and H₂O in the case of gasification. This paper deals with the combustion aspects of the effluent.

It is known that recovery boilers in paper industries utilize black liquor that is concentrated to better than 65% to ensure good combustion. The effluent from the distillery having 10–11% solids can be treated similarly if it is concentrated to better than 65%. This provides the motivation to study the combustion characteristics of concentrated effluents. If gasification is to be pursued or incineration of lower

concentration effluents is to be handled, it may be imperative to deal with one zone of combustion with higher concentration effluents supporting the combustion of lower concentration effluents. It is for this reason that it is useful to understand the behavior of dried effluents. Two limiting conditions are considered for study in this work. The first is the simpler case of dried solid sphere combustion. This is similar to wood sphere combustion, the difference being the presence of a large amount of inorganic material (~38%), which is a significant heat sink in these quantities; it could also be catalytic. Wood has lignin, which is more difficult to pyrolyze compared with sugar. The second part is the study of tiny drops of concentrated effluent to assist in understanding better combustion of sprayed effluent material.

Experimental Procedure

The basic material used for the dry sphere experiments was effluent concentrated to 70%, having the appearance of thick, heavy oil or grease. Since it is difficult to make spheres with this substance, the effluent was further concentrated to 85% by slow convective heating at temperatures between 50 and 110 °C. Loss of sphericity was corrected, and finally, the material was dried in a vacuum desiccator containing silica gel and phosphorus pentoxide. Remaining moisture was gradually removed in a hot air oven at a slow rate. Finally, the spheres were heated at 110 °C for 24 h, before being stored in cooled conditions in a vacuum desiccator. Prior to each experiment, the samples were characterized for weight, and the average diameter was calculated from measurement across three orthogonal axes. The density of the samples varied from 650 to 800 kg/m³.

The samples were mounted on three adjustable nichrome prongs and then inserted into the furnace, which was maintained at a fixed temperature. The combustion process was timed from the moment the sample was introduced into the furnace. Series of experiments were conducted separately, and the variation of surface temperature with time was recorded. Here, the sample was held taut between nichrome prongs held in a horizontal position along with a thermocouple junction (Pt–Pt13%Rh, 50 µm coated with cerium oxide of 0.2 µm in thickness) touching the surface under small tension so as to be firmly in position. In the case of droplets of 65% concentration, the droplets of 0.5–3 mm in diameter were suspended around the 50-µm thermocouple bead and introduced into the furnace. Apart from the transient temperature data, the combustion process was captured on a video camera for subsequent analysis. The initial droplet diameter was measured using a traveling microscope, and further changes in diameter due to the hot ambience was measured using video recording of the event where the drop size

was compared with the predetermined length of a wire fixed on a holder located in the same plane as the suspended droplet.

Experimental Observations

It was found that a minimum ambient gas temperature was required to achieve ignition (flaming of volatiles in gas phase). This feature depends on the dry effluent sphere diameter; large spheres ignite at as low as 530 °C. At temperatures below this, there would be smoldering combustion, with no visible flame. Most of the experiments were performed at 700 °C for which ignition occurred for all dry effluent spheres with diameter in excess of 2 mm. The combustion process was observed to be consisting of two phases. In the first phase, a gaseous flame envelopes the sphere as in the case of liquid droplet combustion. The source of fuel for the flame comes from the gases due to pyrolysis of the solid material. During the flaming process, a lot of fumes were observed to be issuing from the burning zone. This stopped at or a little after the end of flaming. It is suggested that the fumes seen must be the inorganics being carried away by the volatiles. The change in diameter is negligible at the end of this flaming phase. The second phase has no gaseous flame, and the char burns by heterogeneous oxidation with gradual growth of ash layer from the outer surface. The material maintained sphericity throughout the combustion. In some cases of large diameter spheres, flaming and char glowing overlapped for a small duration due to possible incomplete devolatilization in some regions. Some of the observations are qualitatively similar to those made by Mukunda et al. [1] for wood spheres and those made by Kuwata et al. [2] for cellulose spheres.

Combustion of 65% effluent droplets also exhibits the two phases of combustion. However, the minimum ignition temperature was observed to be more than 900 °C for a drop of diameter 2.5 mm. For these cases, water expulsion is accompanied by an increase in diameter of about 40–45%. In this process, the escaping volatiles create a large number of very small pores.

One question that became important was to determine if the condensed-phase pyrolysis or phase transformation was exothermic, as in the case of wood. To explore this hypothesis, thermogravimetric analysis was carried out on the samples of effluent char. These showed clear exotherms at 450 and 560 °C, indicating exothermicity of the decomposition process much like wood.

The Mathematical Model

The primary assumption made in the model is that the conversion process is one-dimensional. Taking

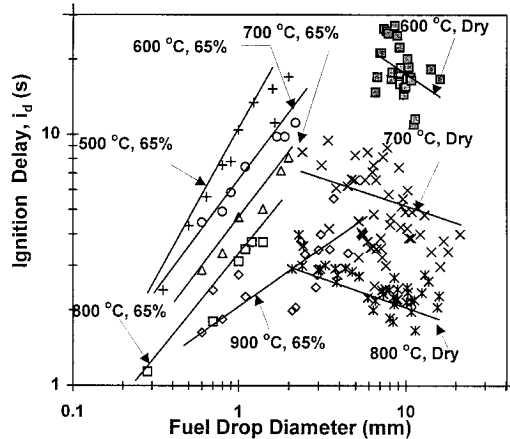


FIG. 1. Variation of ignition time with the liquid drop diameter (65% concentration) and dried spheres of effluent material at 500, 600, 700, 800, and 900 °C.

this assumption, the processes taking place during flaming are the combustion of volatiles, as for wood spheres—diffusion-limited gas-phase combustion, modeled by the Burke–Schumann theory with appropriate initial and boundary conditions [1]. As has been discussed above, the mathematical framework developed in Ref. 1 can be directly utilized in the treatment of the flaming process and, therefore, will not be addressed here.

The processes taking place during combustion of porous char spheres are similar to those treated in Ref. 3 involving the diffusion and convection of the species and energy in the porous medium and the heterogeneous reaction between the gaseous species and the char. These are modeled in the present analysis using the unsteady spherically symmetric, one-dimensional conservation equations.

The primary difference between wood spheres and dry effluent spheres is the amount of inorganics—about 1% for wood and 39% for the effluent spheres.

Choice of Parameters

The choices of physical, thermodynamic, and transport properties of dry effluent material and char based on measured and literature information are as follows: For the dry effluent,

$$\rho_c = 730 \text{ kg/m}^3 \quad c_p = 1.40 \text{ kJ/kg K}$$

$$k_c = 2.1 \text{ W/m K} \quad k_g = 0.063 \text{ W/m K}$$

for the char,

$$\rho_c = 1650 \text{ kg/m}^3 \quad r_p(t = 0) = 50 \mu\text{m}$$

$$c_p = 1.25 \text{ kJ/kg K}$$

$$H_c = 32.60 \text{ MJ/kg} \quad k_c = 1.85 \text{ W/m K}$$

$$k_g = 0.071 \text{ W/m K}$$

and rate parameters for the C + O₂ reaction are

$$A_c = 1/150 \quad E_1/R = 1700 \text{ K} \quad E_2/R = 20,000 \text{ K}$$

$$A_f = 0.0875 \text{ mol/m}^2 \text{ s}$$

where k_c is the conductivity of the solid phase at temperatures of 1000–1200 K. The presence of a large amount of inorganic material affects the conductivity of the porous carbon-inorganic matrix. It must be emphasized that the char is composed of nearly equal amounts of carbon and inorganic matter—oxides, chlorides, sulfides, and sulfates of potassium, sodium, magnesium, and calcium. The thermal conductivity data of several inorganics and char were examined from standard literature. These indicate to values anywhere between 0.5 and 2 W/m K. The conductivity of porous carbon is also within the same range at high temperature. In light of this and the known significant influence of thermal conductivity [3], it was decided to choose a value to match the burn time at one point. This value is 1.25 W/m K. The initial radius of the pore is obtained from Ref. 4, where wood char was used for measurements. The parameters in the kinetic expression used presently were not altered from those of wood char [5]. The rate of the backward reaction k_2 is obtained from the appropriate equilibrium constants. The emissivity of the sphere surface, used for radiant heat loss calculation, is taken as 0.95.

Results and Discussion

Figure 1 shows the dependence of ignition delay (i_d) on the diameter of the spherical particle. Results for both the concentrated liquid and the dried spheres are shown in the figure. In the case of liquids, there is increase in delay with drop diameter much like nonvolatile droplets [6]. The ignition delay decreases with increase in ambient temperature, as can be expected. In the case of dry spheres, even though there is scatter of data, it appears reasonable to conclude that the delay time is nearly independent of the size or that there is a slight decrease in the delay with increase in size. Earlier experimental data on highly volatile fuels and nonvolatile fuels, as well as their blends [6,7], suggest that the decreasing trend of ignition delay with size is due to fuels that are more volatile. The dry effluent appears similar to volatile fuels with regard to ignition delay. Similar results are also reported by Ragland and Weiss [8] and Boukara et al. [9] for bituminous coal.

Figure 2 shows the dependence of ignition features on a diameter vs. ambient temperature plot. A clear boundary between the flaming and nonflaming zone is noticeable. Again, this feature has been

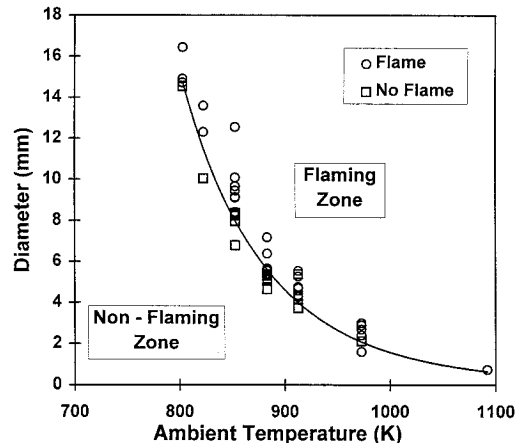


FIG. 2. Boundary between ignition and no ignition on temperature vs. sphere diameter plot for dried effluent.

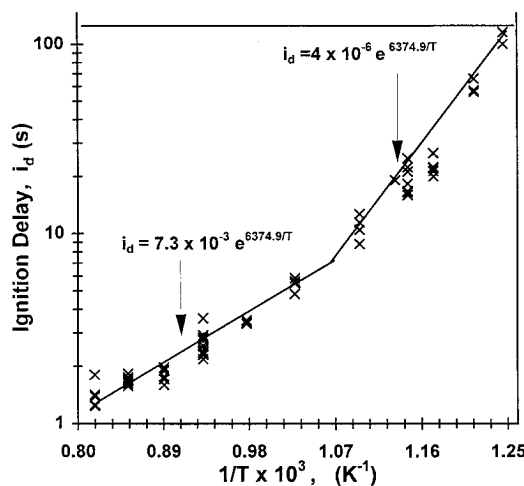


FIG. 3. Ignition delay vs. temperature for different diameter spheres of dried effluent.

observed earlier by Takei et al. [6] and explained to be due to a competition between chemical heat re-

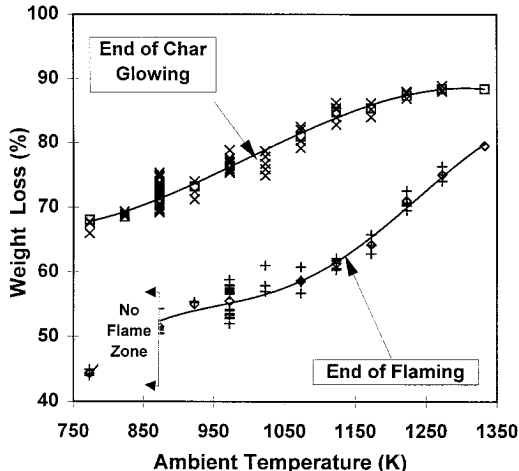


FIG. 4. Plot of weight lost by dried effluent spheres of various diameters at different ambient temperatures at the end of flaming and char glowing.

lease rate and diffusion of reactants in space. For the case of dry effluent spheres, ignition delay correlates well with temperature following the Arrhenius law, as can be noted from Fig. 3.

Figure 4 shows the weight loss at the end of flaming as well as glowing. The data are constructed from a large number of tests for flaming and glowing separately. The portion marked "no flame zone" shows the domain below which only smoldering combustion takes place. Typical weight loss at the end of flaming increases from 50% to as high as 80% at 1330 K. Since an analysis of the dry samples indicated an organic content of 60–65%, the observation on weight loss noted above implies loss of a fair amount of inorganics along with organics during the flaming process. This is supported by the physical observation of fumes exuding from the burning sphere. In order to understand this behavior, the samples from the original effluent, as well as the char and the ash from experiments at various

TABLE I
Analysis of the initial sample, char, and ash for experiments at different temperatures

Nature of Material	Temperature (K)	Initial Sample (g)	Char (g)	Ash (g)	Loss during Flaming (%)	Loss during Glowing (%)
Organics	773	60.3	27.9	0.6	53.6	97.7
Inorganics	773	39.7	26.6	30.2	33.1	-13.6
Organics	873	60.3	24.9	0.6	59.7	97.8
Inorganics	873	39.7	23.1	26.4	41.9	-14.3
Organics	973	60.3	22.7	0.5	62.2	97.9
Inorganics	973	39.7	21.6	22.8	45.5	-5.5

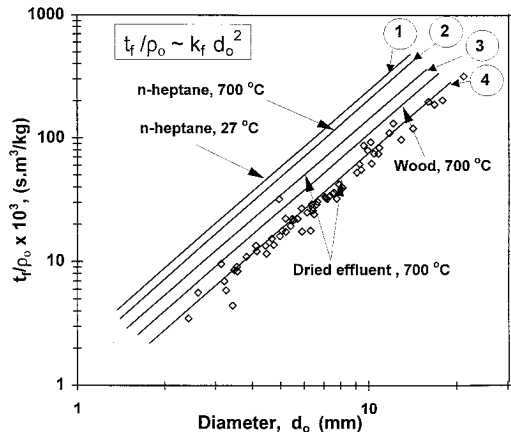


FIG. 5. Flaming time vs. diameter for dried effluent material at different temperatures. Results for *n*-heptane and dried wood sample are also shown.

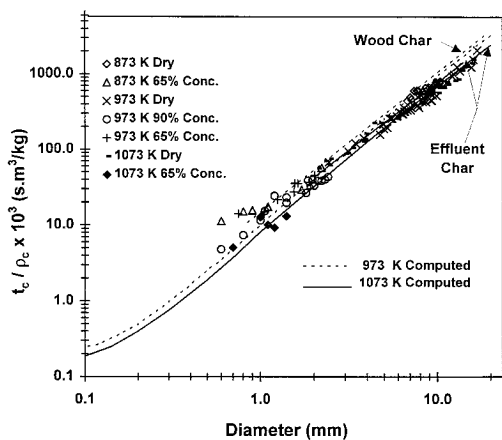


FIG. 6. Glowing time vs. diameter for concentrated liquid droplets and dried effluent at various temperatures. Also shown are the results for wood char. Comparison with model prediction included in the figure.

temperatures, were subjected to chemical analysis. The results of the analysis of original material, char, and ash are shown in Table 1.

The material lost during flaming increases from 53.6 to 62.2% for an ambient temperature rise from 500 to 700 °C. This increase will be far more at higher temperatures, as indicated in Fig. 4. One of the curious aspects of the results is that the amount of inorganics found in ash is more than in char. More careful examination showed that the sulfate content in the char is much less than that either in the ash or in the original effluent. A chemical analysis showed sulfides in the char, which were absent both in the original effluent and in the ash. Hence, it is

inferred that part of the metal sulfates present in the original effluent were reduced to sulfides in the high-temperature-reducing atmosphere in the presence of carbon during flaming combustion [10] and converted back to sulfates during glowing combustion. Other salts also might behave similarly, causing a net increase in the amount of inorganics during the char glowing phase.

The weight loss during char combustion is about 17–20% of the original weight of the sample for temperatures up to 1150 K, and decreases to 7% at 1330 K. It is therefore reasonable to assume that the weight loss during char combustion is constant below about 1150 K.

The data of flaming time, normalized by initial density with diameter (dried sample), are presented in Fig. 5 along with similar data for wood spheres [1] and *n*-heptane [7] for comparison purposes at an ambient temperature of 700 °C on a log-log plot. The flaming time normalization with density is to account for variations in density that occurs in the process of making dry effluent spheres, and the expectation that the combustion time varies linearly with density. Curves 1 and 2 are for *n*-heptane burned at ambient temperatures 27 and 700 °C, respectively. Curve 2 for 700 °C is presented to exhibit a comparison with dried effluent combustion and is obtained using standard liquid droplet combustion calculations, taking into account burning constant dependence on thermodynamic and transport properties. Curves 3 and 4 are for effluent burned at 700 °C. Curve 3 is obtained by normalizing burn time with density that is equivalent to 60% fuel mass, which devolatilized during the flaming process, and curve 4 is normalized with initial density of the dried effluent. A curve fit to this data is of the form $t_f \sim d_0^2$, indicating diffusion-dominated combustion. As can be seen, flaming time in the case of *n*-heptane is larger since it gets completely consumed with zero diameter and zero weight, unlike that for effluent and wood. These data can be interpreted in another way. If one constructs a nondimensional burn time, τ , defined by

$$\tau = t_f \frac{k_w}{\rho_w c_{pw}} \frac{1}{d_0^2} \quad (1)$$

where the quantities subscripted by *w* refer to solid phase, the quantity τ works out to be 0.117 for effluent and 0.105 for wood. For *n*-heptane, it is about 0.1. Thus, this quantity seems to give a value that is fairly constant for all these substances.

Figure 6 presents the experimental data of char glowing time normalized with char density of the dried effluent, effluent with 65% concentration of solids and wood char, and with diameter d_0 for combustion in air under ambient temperatures of 700, 800, and 900 °C. Computations of char combustion in air with the data indicated earlier are shown in

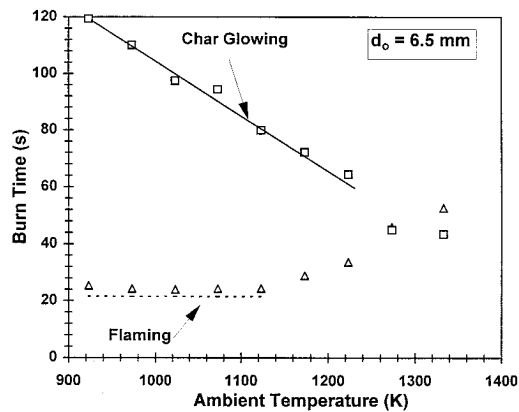


FIG. 7. Flaming and char glowing time as a function of ambient temperature for dried effluent.

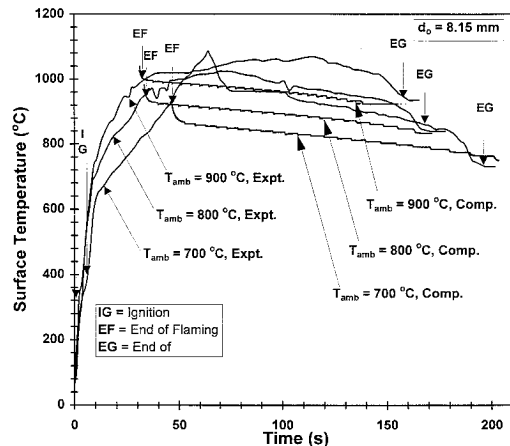


FIG. 8. Surface temperature variation with time.

the same figure by lines. The slope of the line gives the exponent in $t/\rho_c \sim d_0^m$ as $m = 2$. The line remains straight up to a lower end diameter of 1 mm. Below this, the line becomes curved, the slope decreasing with decrease in diameter, indicating increasing reaction control at lower diameters.

Figure 7 shows the burn time (both flaming and glowing) of a 6.5-mm-diameter sphere as a function of temperature. The computed flaming and glowing times are also shown in the figure. As discussed earlier, there is a small increase in the mass loss during the flaming period as temperature increases, which is compensated by increase in heat flux, and as a result, the flaming time remains nearly independent of ambient temperature up to 1150 K. Beyond this temperature, the percentage weight loss increases rapidly with ambient temperature (Fig. 4), causing increase in flaming time. Char glowing time decreases with ambient temperature because of the in-

crease in reaction rate and to a certain extent due to increase in the transport properties. Even though the oxygen–carbon reaction is essentially diffusion controlled and consequently insensitive to changes in the rate constants, the increase in the rate of the reduction reaction between CO_2 and carbon causes a decrease in the overall char glowing time with increasing ambient temperature. It is observed from the computational results that as the temperature increases, the CO_2 fraction decreases, and CO fraction increases at the center of the sphere, indicating increasing $\text{C}-\text{CO}_2$ reaction rate.

The result of the thermal probing is presented in Fig. 8, which contains the surface temperature variation with time during combustion for a sample of 8.15 mm in diameter at 700, 800, and 900 °C. After ignition, there is a sharp temperature rise followed by a slow rise in temperature until the peak. The peak in temperature is observed during active char glowing since the reaction front is shifted to the surface where ambient oxygen diffuses into the porous char, resulting in char combustion. This is followed by a gradual fall in surface temperature until the end of char glowing. Predictions of the temperature profile during char combustion, extracted from the model calculations, are also presented in Fig. 8. The difference in the two results is about 100 K in all three cases. The possible reason for this is that the inorganic compounds in the ash catalyze the exothermic reactions in the gas phase (oxidation of CO), causing higher temperatures in the ash layer.

Concluding Remarks

This paper has presented results of the combustion behavior of concentrated and dried distillery effluent spheres. The ignition time increases linearly with diameter for concentrated effluent and is nearly independent of size for dried effluent. The flaming behavior is similar to that for liquid droplets (*n*-heptane) but with a faster burn rate; the burn rate compares with a wood sphere when suitably nondimensionalized. Char burn rate is again diffusion controlled down to very small diameter spheres. The behavior is modeled using one-dimensional, spherically symmetric conservation equations, and the model predicts most of the features of char combustion satisfactorily.

REFERENCES

- Mukunda, H. S., Paul, P. J., Shrinivasa, U., and Rajan, N. K. S., *Twentieth Symposium (International) on Combustion*, The Combustion Institute, Pittsburgh, 1984, pp. 1619–1628.
- Kuwata, M., Stumbar, E., and Essenhigh, R. H., *Twelfth Symposium (International) on Combustion*,

- The Combustion Institute, Pittsburgh, 1969, pp. 663–674.
- 3. Dasappa, S., Paul, P. J., Mukunda, H. S., and Shrinivas, U., *Chem. Eng. Sci.* 49:223–232 (1994).
 - 4. Groeneveld, M. J., “The co-current moving bed gasifier,” Ph.D. Thesis, Twente University of Technology, Netherlands, 1980.
 - 5. Blackwood, J. D. and Ingeme, A. J., *Aust. J. Chem.* 13:194–209 (1960).
 - 6. Takei, M., Tsukamoto, T., and Nioka, T., *Combust. Flame* 93:149–156 (1971).
 - 7. Kumagai, S., Sakai, T., and Okajima, S., *Thirteenth Symposium (International) on Combustion*, The Combustion Institute, Pittsburgh, 1971, pp. 779–785.
 - 8. Ragland, K. W. and Yang, J., *Combust. Flame* 60:285–297 (1985).
 - 9. Boukara, R., Gadiou, R., Gilot, P., Delfosse, L., and Prado, G., *Twenty-Fourth Symposium (International) on Combustion*, The Combustion Institute, Pittsburgh, 1992, pp. 1127–1133.
 - 10. Brown, G. H. and Sallee, E. M., *Quantitative Chemistry*, Prentice-Hall, Englewood Cliffs, NJ, 1963.